A Theoretical Model for the Generation of Kinetic Alfvén Waves in the Earth's Magnetosphere by Ion Beam and Velocity Shear

Article *in* URSI Radio Science Bulletin · January 2020

DOI: 10.23919/URSIRSB.2019.8956140

CITATIONS
9

READS
217

3 authors:

Krushna Chandra Barik
University of California, Berkeley
9 PUBLICATIONS **54** CITATIONS

SEE PROFILE

S. V. Singh
Indian Institute of Geomagnetism
221 PUBLICATIONS **5,561** CITATIONS

SEE PROFILE

G. S. Lakhina
Indian Institute of Geomagnetism
313 PUBLICATIONS **6,429** CITATIONS

SEE PROFILE

A Theoretical Model for the Generation of Kinetic Alfvén Waves in the Earth's Magnetosphere by Ion Beam and Velocity Shear

K. C. Barik, S. V. Singh, and G. S. Lakhina

Indian Institute of Geomagnetism
Navi Mumbai 410218, India
E-mail: kcbarik17@gmail.com

Abstract

A generation mechanism for kinetic Alfvén waves (KAWs) by ion-beam and velocity shear is discussed. For this, a three-component plasma model, consisting of cold background ions, hot electrons, and hot ion beams is considered. The model is very general in the sense that all of the three species have drifting Maxwellian distributions, nonuniform streaming, and velocity shear, and can be applied to magnetospheric regions where velocity shear is present. The effects of the ion beam alone and the combined effect of the ion beam as well as the velocity shear in exciting the kinetic Alfvén waves are discussed. It is found that the ion beam alone can excite these kinetic Alfvén waves. However, in the presence of an anti-parallel ion beam and positive shear, the wave growth is much larger as compared to the ion-beam case alone. For a set of plasma parameters, waves are excited for $\lambda_B < 1$ for the case of the ion beam alone, whereas for the combined case (an anti-parallel ion beam and positive velocity shear), these waves are excited for $\lambda_B > 1$. The present model is applied to the polar cusp/auroral region of the Earth's magnetosphere, and it can explain several characteristic properties of the observed ultra-low-frequency waves. The mechanism presented here can excite the kinetic Alfvén waves up to a frequency of ≈ 65 mHz, which can explain the ultra-low-frequency waves observed in the auroral/polar cusp region.

1. Introduction

Kinetic Alfvén waves (KAWs) are low-frequency electromagnetic waves that propagate nearly perpendicular to the ambient magnetic field, and have an electric-field component along the ambient magnetic field. The acceleration of charged particles in space plasmas is related to the presence of parallel electric fields. Due to the presence of a parallel electric field, kinetic Alfvén waves play a major role in the transfer of energy to particles and auroral acceleration of the electrons [1-5]. In the low-β plasmas, this parallel electric field arises in the magneto-hydrodynamic (MHD) waves under two aspects. First, when electron inertia is taken into account, the shear Alfvén waves will come into the picture and will satisfy conditions in a region where with β being the (thermal pressure/magnetic pressure) [3]. Second, when the ion gyro radius is taken into account, kinetic Alfvén waves will play a major role and satisfy conditions in a region where $\beta \gg m_e/m_i$ [6]. At the auroral altitudes of 4-5 R_E, where is the radius of the Earth, the shear Alfvén wave plays a major role [7], and beyond that, the kinetic Alfvén waves are important. Observationally, kinetic Alfvén waves appear as broadband enhancements in electric and magnetic field wave power that become increasingly electrostatic at higher frequencies [8-11]. These waves have been reported inside the plasmasphere in conjunction with, and modulated by, ultra-low-frequency (ULF) oscillations driven by an impulsive solar-wind pressure enhancement, and are identified as Doppler-shifted kinetic Alfvén waves. Furthermore, kinetic Alfvén waves may significantly impact particle dynamics in the inner magnetosphere through enhanced ion transport and heating [2, 12]. Observations carried out onboard the S3-3, DE1, AUREOL 3, VIKING, CLUSTER, THEMIS, Van Allen Probes, and MMS spacecraft have given evidence for intense electromagnetic turbulence in the solar wind and magnetosphere [13-20].

Ultra-low-frequency waves have been observed in various regions of the Earth's magnetosphere, e.g., the magnetopause, magnetosheath, plasma-sheet boundary layer (PSBL), polar cusp, and on auroral field lines for decades [8, 21-26]. These ULF waves can be generated

by several mechanisms [8, 21, 22, 24]. Instabilities/waves such as the Kelvin-Helmholtz (K-H) instability [21, 27, 28], kinetic Alfvén waves [1, 3, 5, 29-31], field-line resonance [28], etc., are some of the phenomena that can explain the generation of ULF waves. More recent observations in the terrestrial magnetosphere and reconnection region have shown that kinetic Alfvén waves facilitate the generation of ULF waves and wave-particle energy exchange [20, 32]. Lakhina [31] discussed the excitation of kinetic Alfvén waves by velocity shear and explained the observed generation of ULF waves by kinetic Alfvén waves. Ion beams have also been observed in various regions of the magnetosphere such as the plasma-sheet boundary layer, polar cusp, auroral zone, etc. [24, 27]. Here, we are proposing a three-component plasma model for the excitation of kinetic Alfvén waves by ion-beam and velocity shear as a possible mechanism for the generation of ULF waves in the Earth's magnetosphere. The combined effect of ion-beam and velocity shear in exciting the kinetic Alfvén waves for resonant instability has been studied. This model is able to explain some of the observed characteristics of ULF waves in the magnetosphere.

2. Theoretical Model for Kinetic Alfvén Waves Excited by Ion-Beam and Velocity Shear

A three-component theoretical plasma model is considered, having background ions, beam ions, and electrons as its species. All the three species have nonuniform streaming along the ambient magnetic field $\mathbf{B}_0 = B_0\hat{z}$, where $X = x + v_y/\omega_{cj}$, $\omega_{cj} = \dfrac{q_j B_0}{m_j c}$ is the gyro frequency of the jth species, q_j and m_j are the charge and mass of the jth species, c is the light speed, and the subscript is e, i, or B for electrons, ions, and beam ions, respectively. The equilibrium charge neutrality is obtained from the relation , where N_j represents the number density of the jth species. To proceed further, we have assumed a drifting Maxwellian distribution, given by

$$f_{0j} = \left(\pi\alpha_j^2\right)^{-3/2} N_j \exp\left[-\left\{v_\perp^2 + \left[v_\parallel - V_j(X)\right]^2\right\}\Big/\alpha_j^2\right] \qquad (1)$$

where $v_\perp = \sqrt{v_x^2 + v_y^2}$ and $v_\parallel = v_z$ define the perpendicular and parallel velocity components with respect to the ambient magnetic field, $\alpha_j = \sqrt{\dfrac{2T_j}{m_j}}$ is the thermal speed of the jth species, and T_j is the temperature of the jth species.

Since we are assuming a low-beta plasma (thermal pressure/magnetic pressure) for our study, the wave is assumed to be magnetically incompressible. This means that the z component of the wave's magnetic field, B_z, is zero. This fact allows us to use the two electric potentials to describe the wave's electric field, as done by Hasegawa [1]. The electric field of the electromagnetic wave can thus be written as

$$\mathbf{E} = -\nabla_\perp\phi + E_\parallel\hat{z}\,, \qquad (2)$$

where $E_\parallel = -\nabla_\parallel\psi$. The basic equations used for our calculations are Poisson's equation and the z component of Ampere's law. Respectively, they are given by

$$-\nabla_\perp^2\phi + \frac{\partial E_\parallel}{\partial z} = 4\pi\sum_j e_j n_j\,, \qquad (3)$$

$$\frac{\partial\nabla_\perp^2\phi}{\partial z} + \nabla_\perp^2 E_\parallel = \frac{4\pi}{c^2}\frac{\partial}{\partial t}\sum_j J_{zj}\,. \qquad (4)$$

Here, n_j and J_{zj} are respectively the perturbed number and the z component of the current densities, and can be computed from the expressions

$$n_j = \int d^3v f_{1j}\,, \qquad (5)$$

$$J_{zj} = \int d^3v e_j v_z f_{1j}\,,$$

where f_{1j} is the perturbed distribution function, which can be obtained from the linearized Vlasov's equation using a local approximation ($L_v k \gg 1$). Here, k is the wavenumber and $L_v = V_B\left(dV_B/dx\right)^{-1}$ is the velocity gradient scale length. For this, the perturbation is assumed to be of the form $f_{1j} = \exp(ik_\perp y + ik_\parallel z - i\omega t)$, where ω is the frequency of the wave, and $k_\parallel$ and $k_\perp$ are respectively the parallel and perpendicular components of the wave vector $\mathbf{k}$. The generalized perturbed distribution can now be written as [33, Equation (4.169)]

$$f_1(\mathbf{r},\mathbf{v},t) = -\frac{q}{m}\int_{-\infty}^{t} dt'\left[\mathbf{E} + \frac{(\mathbf{E}\cdot\mathbf{v}')\mathbf{k} - \mathbf{E}(\mathbf{v}'\cdot\mathbf{k})}{\omega}\right]$$

$$\cdot\nabla_{v'} f_0(\mathbf{v}')\, e^{i(\mathbf{k}\cdot\mathbf{r}' - \omega t')} \qquad (6)$$

which has to be integrated along the unperturbed orbits. Following the standard procedure and algebraic manipulations, the perturbed distribution function for low-frequency kinetic Alfvén waves can be written as [31,34]

$$f_{1j} = \frac{e_j}{m_j}\sum_{n=-\infty}^{+\infty}\sum_{m=-\infty}^{+\infty}\frac{e^{i(n-m)\theta}}{\left(k_\parallel v_z - \omega + n\omega_{cj}\right)} J_n(\xi_j) J_m(\xi_j)$$

$$\times\left(k_\perp M_j\phi + k_\parallel L_j\psi\right) \qquad (7)$$

where coefficients M_j and L_j can be expressed as

$$M_j = \left(1-\frac{k_{\|}v_z}{\omega}\right)\left[\frac{\partial f_{0j}}{\partial v_{\perp}}\frac{n\omega_{cj}}{k_{\perp}v_{\perp}}+\frac{1}{\omega_{cj}}\frac{\partial f_{0j}}{\partial x}\right]+\frac{\partial f_{0j}}{\partial v_z}\frac{n\omega_{cj}k_{\|}}{k_{\perp}\omega} \quad (8)$$

$$L_j = \frac{k_{\perp}v_z}{\omega}\left[\frac{\partial f_{0j}}{\partial v_{\perp}}\frac{n\omega_{cj}}{k_{\perp}v_{\perp}}+\frac{1}{\omega_{cj}}\frac{\partial f_{0j}}{\partial x}\right]+\left(1-\frac{n\omega_{cj}}{\omega}\right)\frac{\partial f_{0j}}{\partial v_z} \quad (9)$$

Here, $J_n(\xi_j)$ and $J_m(\xi_j)$ are the Bessel functions of the order n and m, respectively, with the arguments $\xi_j = \left(k_{\perp}v_{\perp}/\omega_{cj}\right)$. For the calculation of velocity integrals, we use cylindrical coordinates, i.e., $\mathbf{v} = \left(v_{\perp}, \theta, v_{\|}\right)$, where θ represents the angular coordinate of the velocity vector. Substituting f_{1j} from Equation (7) into Equation (5) and evaluating the integrals, we obtain the perturbed number density, n_j, and the parallel component (z component) of the current density, J_{zj}. Furthermore, these number and current densities are substituted into Equations (3) and (4), respectively, to get the following:

$$\begin{pmatrix} D_{11} & D_{12} \\ D_{21} & D_{22} \end{pmatrix}\begin{pmatrix} \phi \\ \psi \end{pmatrix} = 0 \quad (10)$$

where the coefficients are given by the expressions

$$D_{11} = k_{\perp}^2\left[1+\sum_j \frac{2\omega_{pj}^2}{k_{\perp}^2\alpha_j^2}\frac{\bar{\omega}}{\omega}\left(1-b_j\right)\right], \quad (11)$$

$$D_{12} = k_{\|}^2\left[1-\sum_j \frac{\omega_{pj}^2 b_j}{k_{\|}^2\alpha_j^2}Z'\left(\frac{\bar{\omega}}{k_{\|}\alpha_j}\right)\left(1-S_j\frac{k_{\perp}}{k_{\|}}\right)\right], \quad (12)$$

$$D_{21} = k_{\|}k_{\perp}^2\left[1+\sum_j \frac{\omega_{pj}^2 b_j}{c^2k_{\perp}^2}S_j\frac{k_{\perp}}{k_{\|}}\right], \quad (13)$$

$$D_{22} = -k_{\|}k_{\perp}^2\left\{1+\sum_j \frac{\omega_{pj}^2}{c^2k_{\perp}^2}\left[\frac{b_j\omega^2}{k_{\|}^2\alpha_j^2}Z'\left(\frac{\bar{\omega}}{k_{\|}\alpha_j}\right)\left(1-S_j\frac{k_{\perp}}{k_{\|}}\right)+S_j\frac{k_{\perp}}{k_{\|}}\right]\right\}, \quad (14)$$

where $\omega_{pj} = \left(\frac{4\pi N_j e_j^2}{m_j}\right)^{1/2}$ is the plasma frequency, $\bar{\omega} = \left(\omega - k_{\|}V_j\right)$ is the Doppler-shifted frequency of the jth species, and $b_j = I_0\left(\lambda_j\right)\exp\left(-\lambda_j\right)$, where $I_0\left(\lambda_j\right)$ is the zeroth-order modified Bessel function. The coefficients D_{ij} are obtained by assuming low-frequency waves ($\omega^2 \ll \omega_{cj}^2$) propagating nearly perpendicular to $\mathbf{B}_0$, i.e., $k_{\|}^2 << k_{\perp}^2$. We get the following generalized dispersion relation from Equation (10) by equating the determinant of the coefficients of ϕ and ψ to zero:

$$1+\sum_j \frac{\omega_{pj}^2}{k^2\alpha_j^2}\left[\frac{2\bar{\omega}}{\omega}\left(1-b_j\right)-b_j\left(1-S_j\frac{k_{\perp}}{k_{\|}}\right)Z'\left(\frac{\bar{\omega}}{k_{\|}\alpha_j}\right)\right]$$

$$+\sum_j \frac{2\omega_{pj}^2}{k^2\alpha_j^2}\frac{\bar{\omega}}{\omega}\left(1-b_j\right)$$

$$\sum_j \frac{\omega_{pj}^2}{c^2k_{\perp}^2}\left[\frac{b_j\omega^2}{k_{\|}^2\alpha_j^2}Z'\left(\frac{\bar{\omega}}{k_{\|}\alpha_j}\right)\left(1-S_j\frac{k_{\perp}}{k_{\|}}\right)+S_j\frac{k_{\perp}}{k_{\|}}\right]$$

$$-\sum_j \frac{\omega_{pj}^2 b_j}{k^2\alpha_j^2}\left(1-S_j\frac{k_{\perp}}{k_{\|}}\right)Z'\left(\frac{\bar{\omega}}{k_{\|}\alpha_j}\right)\sum_j \frac{\omega_{pj}^2 b_j}{c^2k_{\perp}^2}S_j\frac{k_{\perp}}{k_{\|}} = 0. \quad (15)$$

3. Resonant Instability of Kinetic Alfvén Waves

In this section, we study the resonant instabilities of the kinetic Alfvén waves excited by hot-ion beams and velocity shear. The dispersion relation is here restricted to a hot-ion beam with drift velocity V_B and shear in the flow of $S = S_B$, whereas other species have $V_i = 0 = V_e$ $S_i = 0 = S_e$. Under the assumptions of a hot-ion beam, $\omega \ll k_{\|}\alpha_e$, $\lambda_e \ll 1$, hot electrons, $\omega \ll k_{\|}\alpha_e$, $\lambda_e << 1$, and cold background ions, $\omega^2 \gg k_{\|}^2\alpha_i^2$, the dispersion relation obtained from Equation (15) is given by

$$\frac{b_i N_i}{N_e}\left[1+a_1-\frac{\omega^2}{k_{\|}^2v_A^2}\frac{N_i}{N_e}\frac{1-b_i}{\lambda_i}Aq_0\right]$$

$$-\frac{\omega^2}{k_{\|}^2c_s^2}\left[C_R'+i\left(1+a_1\right)C_I-\frac{\omega^2}{k_{\|}^2v_A^2}\frac{N_i}{N_e}\frac{1-b_i}{\lambda_i}A\left(C_R+iC_I\right)\right]$$

$$=\frac{2\omega^2}{k_{\|}^2\alpha_i^2}\frac{\left(1-b_i\right)N_i}{N_e}, \quad (16)$$

where

$$a_1 = \frac{N_B}{N_e}\frac{\beta_B b_B}{2\lambda_B} S\frac{k_\perp}{k_\parallel}, \quad (17)$$

$$q_0 = 1 + \frac{N_B}{N_i}\frac{m_i}{m_B}\frac{Sk_\perp}{b_i k_\parallel}, \quad (18)$$

$$A = 1 + \frac{N_B}{N_i}\frac{T_i}{T_B}\frac{\bar{\omega}}{\omega}\frac{(1-b_B)}{(1-b_i)}, \quad (19)$$

$$C_R = 1 + \frac{N_B}{N_e}\frac{T_e}{T_B} b_B\left(1 - S\frac{k_\perp}{k_\parallel}\right), \quad (20)$$

$$C_R' = 1 + \frac{N_B}{N_e}\frac{T_e}{T_B}\left[b_B\left(1-\frac{\bar{\omega}}{\omega}\right) + \left(\frac{\bar{\omega}}{\omega} - b_B S\frac{k_\perp}{k_\parallel}\right)\right] + a_1 C_R \quad (21)$$

$$C_I = \sqrt{\pi}\,\frac{\omega}{k_\parallel \alpha_e}\left[\exp\left(-\frac{\omega^2}{k_\parallel^2\alpha_e^2}\right) + b_B\frac{N_B}{N_e}\left(\frac{T_e}{T_B}\right)^{3/2}\left(\frac{m_B}{m_e}\right)^{1/2}\right.$$

$$\left.\frac{\bar{\omega}}{\omega}\left(1 - S\frac{k_\perp}{k_\parallel}\right)\exp\left(-\frac{\bar{\omega}^2}{k_\parallel^2\alpha_B^2}\right)\right]. \quad (22)$$

The expression C_I here represents the damping terms due to hot electrons and beam ions, and $c_s = \left(T_e/m_i\right)^{1/2}$ is the ion acoustic speed, $v_A = \left(B_0^2/4\pi N_e m_i\right)^{1/2}$ is the Alfvén velocity, and $\beta_i = \left(8\pi N_e T_i/B_0^2\right)$ and $\beta_B = \left(8\pi N_e T_B/B_0^2\right)$ are the ion and beam plasma betas, respectively. In the absence of ion beam ($N_B = 0$) and neglecting the damping due to electron and beam ions, we will reach the usual dispersion relation for kinetic Alfvén waves in a two-component plasma, as obtained by Hasegawa and Chen [1] and Lakhina [31]. We can write the general dispersion relation, Equation (16), as a combination of real and imaginary parts:

$$D_R(\omega,k) + iD_I(\omega,k) = 0 \quad (23)$$

where

$$D_R(\omega,k) = \frac{\omega^4}{k_\parallel^4 V_A^4}\left[\frac{N_i}{N_e}\frac{(1-b_i)}{\lambda_i} AC_R\right]$$

$$- g_1\frac{\omega^2}{k_\parallel^2 V_A^2} + \frac{N_i}{N_e}\frac{b_i\beta_i}{2}(1+a_1), \quad (24)$$

$$D_I(\omega,k) = -\frac{\omega^2}{k_\parallel^2 V_A^2}\left[1 + a_1 - \frac{\omega^2}{k_\parallel^2 V_A^2}\frac{(1-b_i)}{\lambda_i}\frac{N_i}{N_e}A\right]C_I, \quad (25)$$

$$g_1 = \left\{C_R' + \frac{N_i}{N_e}(1-b_i)\left[\frac{T_e}{T_i} + \frac{N_i}{N_e}\frac{b_i\beta_i}{2\lambda_i}Aq_0\right]\right\} \quad . (26)$$

The real frequency can be obtained by equating $D_R(\omega,k) = 0$, which contains both shear and beam velocity. In the absence of streaming, $V_B = 0$, and assuming $C_I \approx 0$, one can also obtain the real frequency from Equation (24) for non-resonant instability [31].

The growth/damping rate, γ, of the resonant kinetic Alfvén waves can be obtained from Equations (24) and (25) as

$$\gamma = -\frac{D_I(\omega_r,\mathbf{k})}{\dfrac{\partial D_R(\omega_r,\mathbf{k})}{\partial\omega_r}}$$

$$= \omega_r^2\left[1 + a_1 - \frac{\omega_r^2}{k_\parallel^2 v_A^2}\frac{(1-b_i)}{\lambda_i}\frac{N_i}{N_e}A\right]C_I$$

$$\left\{\omega_r\left[2\left(g_1^2 - 4g_0\right)^{1/2}\right] + V_B\frac{N_B}{N_e}(1-b_B)\right.$$

$$\left.\left[\frac{\omega_r^2}{k_\parallel v_A^2}\frac{T_i}{T_B}\frac{C_R}{\lambda_i} - k_\parallel\frac{T_e}{T_B}\left(1 + \frac{N_i}{N_e}\frac{T_i}{T_e}\frac{b_i\beta_i}{2\lambda_i}q_0\right)\right]\right\}^{-1} \quad (27)$$

where

$$g_0 = \left(\frac{N_i}{N_e}\right)^2\frac{b_i\beta_i}{2}\frac{(1-b_i)}{\lambda_i}(1+a_1)AC_R. \quad (28)$$

This is a general expression for the growth/damping rate of the kinetic Alfvén waves in the presence of ion beam and velocity shear. It has been obtained after making use of the assumption $\omega = \omega_r + i\gamma$, where ω_r is the real frequency and $\gamma \ll \omega_r$ is the growth/damping rate.

The numerical computations were next carried out for real frequency, Equation (24), and growth/damping rate,

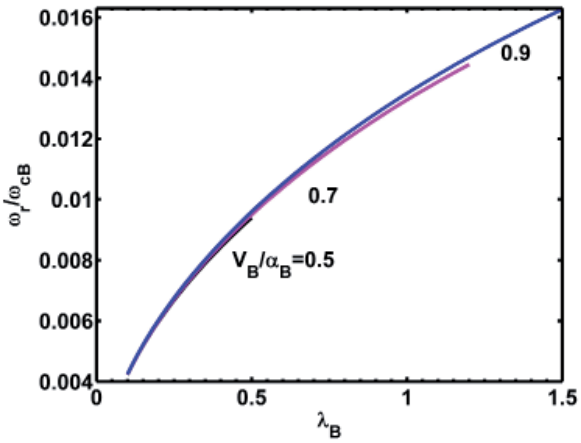

Figure 1a. The resonant instability of kinetic Alfvén waves driven by an ion beam alone: the normalized real frequency, ω_r/ω_{cB}, as a function of $\lambda_B = \frac{k_\perp^2\alpha_B^2}{2\omega_{cB}^2}$ for $\frac{N_B}{N_e} = 0.4$, $\beta_i = 0.001$, $\frac{k_\parallel}{k_\perp} = 0.04$, $S = 0$, and for $\frac{V_B}{\alpha_B} = 0.5$, 0.7, and 0.9, respectively.

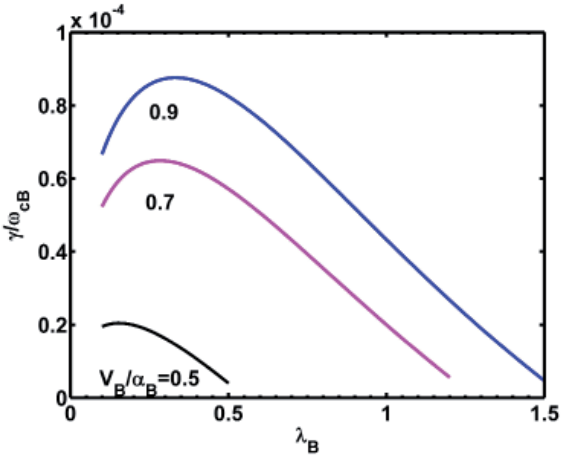

Figure 1b. The resonant instability of kinetic Alfvén waves driven by an ion beam alone: the normalized growth rate, γ/ω_{cB}, as a function of $\lambda_B = \frac{k_\perp^2\alpha_B^2}{2\omega_{cB}^2}$ for $\frac{N_B}{N_e} = 0.4$, $\beta_i = 0.001$, $\frac{k_\parallel}{k_\perp} = 0.04$, $S = 0$, and for $\frac{V_B}{\alpha_B} = 0.5$, 0.7, and 0.9, respectively.

Equation (27), for the relevant plasma parameters. We made sure that all the assumptions that were made in arriving at the theoretical results were satisfied. The normalization procedure that we adopted for our numerical computations were as follows: frequencies, ω_r, were normalized with respect to the cyclotron frequency of the ion beam, ω_{cB}; temperatures with the ion beam temperature, T_B; streaming velocity, V_B, with the thermal speed of the ion beam, α_B. The normalized real frequency and the growth rates of the resonant instability as calculated numerically from Equation (24) and Equation (27), respectively, were plotted against $\lambda_B = k_\perp^2\alpha_B^2/2\omega_{cB}^2$ (the square of the perpendicular wave number normalized with the gyro radius of the beam ions). From the numerical analysis, it was found that for the resonant instability of the kinetic Alfvén waves, $C_R > 0$ and $C_I < 0$ should be satisfied. From the condition $C_R > 0$ an upper limit for the velocity shear was obtained from Equation (20) as

$$S_{max} = \frac{k_\parallel}{k_\perp}\left(1 + \frac{N_e}{N_B}\frac{T_B}{b_B T_e}\right). \qquad (29)$$

The $C_I < 0$ contains terms corresponding to ion beam as well as velocity shear, and hence it was difficult to analytically obtain a combined threshold or upper limit for which growth of the wave occurred. However, in the absence of velocity shear (i.e., $S = 0$), from the condition $C_I < 0$, we obtained an expression for the threshold value of ion beam velocity above which the growth of the waves was possible. This is given by

$$V_{Bth} = \frac{\omega}{k_\parallel}\left[1 + \frac{N_e}{N_B}\frac{1}{b_B}\left(\frac{T_B}{T_e}\right)^{3/2}\left(\frac{m_e}{m_B}\right)^{1/2}\right]. \qquad (30)$$

Figures 1a and 1b represent the normalized real frequency and the normalized growth rate as functions of the square of the normalized perpendicular wave number, $\lambda_B = \frac{k_\perp^2\alpha_B^2}{2\omega_{cB}^2}$, in the absence of velocity shear ($S = 0$). The waves were excited by an ion beam alone. It was observed that when the ion-beam velocity was increased from $\frac{V_B}{\alpha_B} =$ 0.5 to 0.9, the real frequency marginally increased, whereas the growth rate significantly increased. The growth rate first increased up to a certain extent, reached its maximum value, and then fell back. The value of λ_B for which the growth rate was maximum is called λ_{Bmax}. It was observed that with an increase in beam velocity, the λ_{Bmax} shifted towards higher values, i.e., higher wave numbers. The extent of wave numbers for which kinetic Alfvén waves were excited also increased with an increase in ion-beam velocity. It is emphasized here that in the absence of velocity shear, an ion beam alone can excite the kinetic Alfvén waves with reasonable growth rate. The *threshold value* of the beam velocity was found to be $V_B/\alpha_B \approx 0.42$, below which no growth was possible.

In Figures 2a and 2b, plots of normalized real frequency and growth rate in the presence of finite shear ($S = 0.4$) and the ion beam streaming parallel to the ambient magnetic field (positive velocity) are shown. The ion-beam velocity was increased from $\frac{V_B}{\alpha_B} = 0.15$ to 0.45. It was observed that with an increase in beam velocity in the parallel direction, the real frequency increased, although marginally. However, there was slight growth at $\frac{V_B}{\alpha_B} = 0.15$ which diminished with the further increase in ion-beam

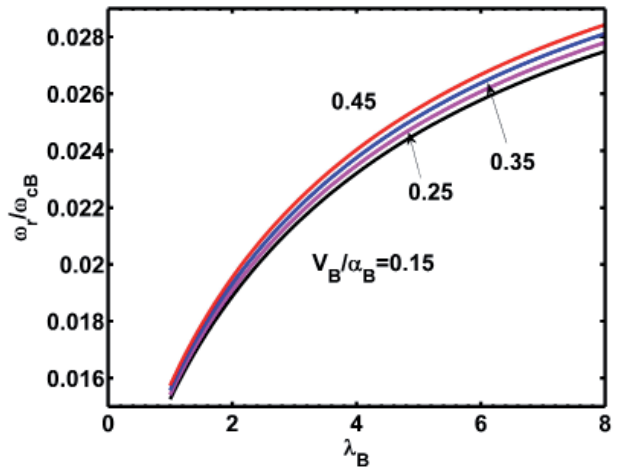

Figure 2a. The resonant instability of kinetic Alfvén waves driven by an ion beam and velocity shear: the normalized real frequency, ω_r/ω_{cB}, as a function of $\lambda_B = \frac{k_\perp^2 \alpha_B^2}{2\omega_{cB}^2}$ for $\frac{N_B}{N_e} = 0.4$, $\beta_i = 0.001$, $\frac{k_\parallel}{k_\perp} = 0.04$ $S = 0.4$, and for $\frac{V_B}{\alpha_B} = 0.15$, 0.25, 0.35, and 0.45, respectively.

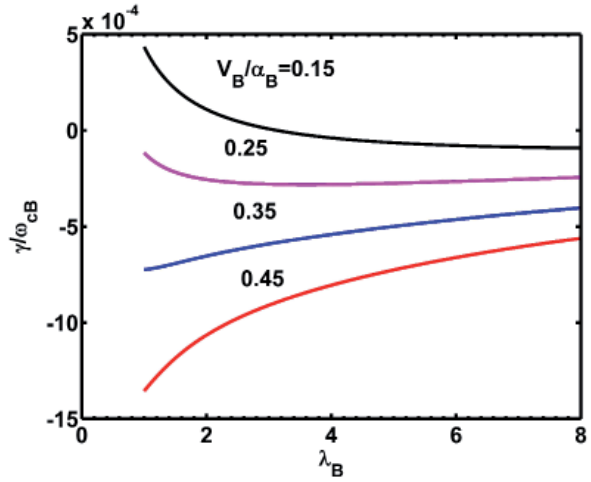

Figure 2b. The resonant instability of kinetic Alfvén waves driven by an ion beam and velocity shear: the normalized growth rate, γ/ω_{cB}, as a function of $\lambda_B = \frac{k_\perp^2 \alpha_B^2}{2\omega_{cB}^2}$ for $\frac{N_B}{N_e} = 0.4$, $\beta_i = 0.001$, $\frac{k_\parallel}{k_\perp} = 0.04$ $S = 0.4$, and for $\frac{V_B}{\alpha_B} = 0.15$, 0.25, 0.35, and 0.45, respectively.

velocity considered here. The waves were thus being damped at higher values of ion-beam velocity. This indicated that positive shear with parallel streaming of ions will have a stabilizing effect on the kinetic Alfvén waves. Due to the damping of the wave, there may be a transfer of energy from the wave to the particles, and hence energy transfer to the particles. Positive velocity shear along with parallel streaming of the ion beam therefore creates a favorable condition for energy transfer to the particles.

In Figures 3a and 3b, the variation of the normalized real frequency and growth rate with the normalized perpendicular wave number in the presence of positive shear ($S = 0.4$) and the ion beam anti-parallel to the ambient magnetic field are shown for $\frac{V_B}{\alpha_B} = -0.15$ to -0.45. With the increase in beam velocity in the anti-parallel direction, the real frequency marginally decreased, whereas the growth rate slightly increased. The growth rate fell off

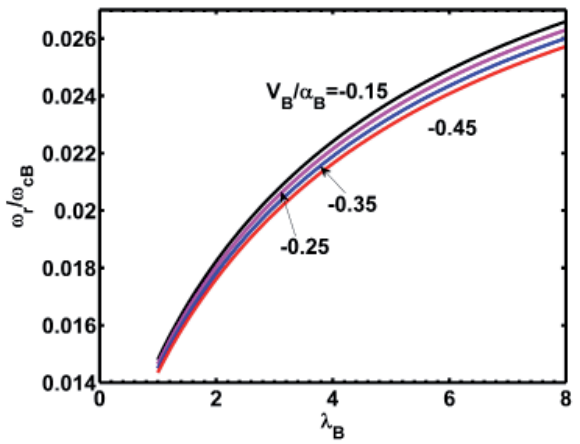

Figure 3a. The resonant instability of kinetic Alfvén waves driven by an ion beam and velocity shear: the normalized real frequency, ω_r/ω_{cB}, as a function of $\lambda_B = \frac{k_\perp^2 \alpha_B^2}{2\omega_{cB}^2}$ for $\frac{N_B}{N_e} = 0.4$, $\beta_i = 0.001$, $\frac{k_\parallel}{k_\perp} = 0.04$ $S = 0.4$, and for $\frac{V_B}{\alpha_B} = -0.15$, -0.25, -0.35, and -0.45, respectively.

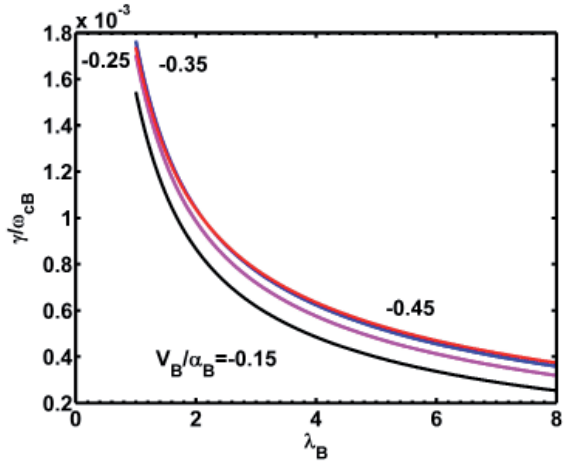

Figure 3b. The resonant instability of kinetic Alfvén waves driven by an ion beam and velocity shear: the normalized growth rate, γ/ω_{cB}, as a function of $\lambda_B = \frac{k_\perp^2 \alpha_B^2}{2\omega_{cB}^2}$ for $\frac{N_B}{N_e} = 0.4$, $\beta_i = 0.001$, $\frac{k_\parallel}{k_\perp} = 0.04$ $S = 0.4$, and for $\frac{V_B}{\alpha_B} = -0.15$, -0.25, -0.35, and -0.45, respectively.

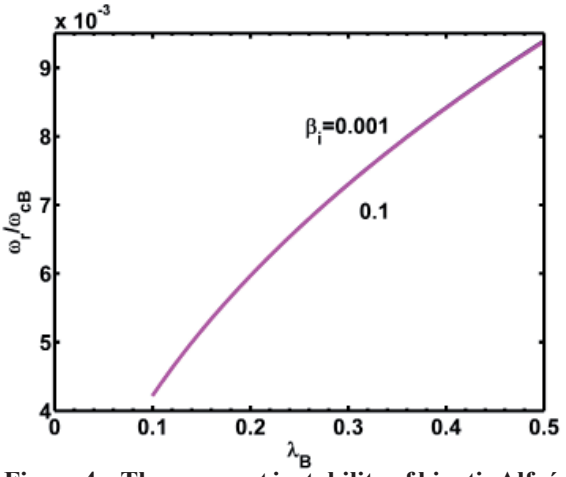

Figure 4a. The resonant instability of kinetic Alfvén waves driven by an ion beam: the normalized real frequency, ω_r/ω_{cB}, as a function of $\lambda_B = \frac{k_\perp^2 \alpha_B^2}{2\omega_{cB}^2}$ for $\frac{N_B}{N_e} = 0.4,$, $\frac{k_\parallel}{k_\perp} = 0.04$, $\frac{V_B}{\alpha_B} = 0.5$, $S = 0.0$, and for $\beta_i = 0.001$ and 0.1, respectively.

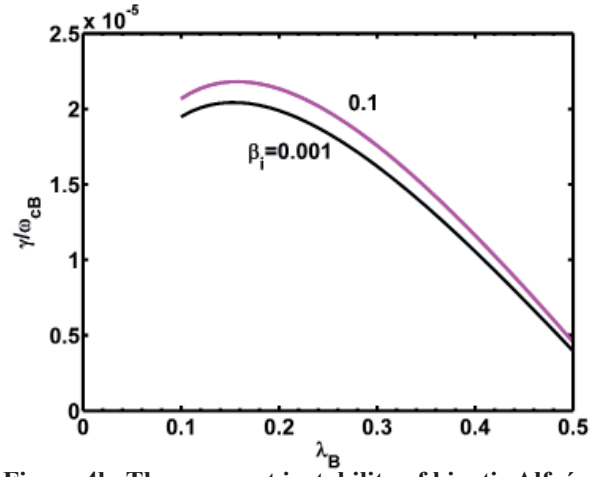

Figure 4b. The resonant instability of kinetic Alfvén waves driven by an ion beam: the normalized growth rate, γ/ω_{cB}, as a function of $\lambda_B = \frac{k_\perp^2 \alpha_B^2}{2\omega_{cB}^2}$ for $\frac{N_B}{N_e} = 0.4,$, $\frac{k_\parallel}{k_\perp} = 0.04$, $\frac{V_B}{\alpha_B} = 0.5$, $S = 0.0$, and for $\beta_i = 0.001$ and 0.1, respectively.

sharply with λ_B. The growth rate was significantly higher than for the case of the ion beam alone (Figure 1b) and for the ion beam and positive velocity shear (Figure 2b). This indicated that an ion-beam streaming anti-parallel to the ambient magnetic field in the presence of a finite shear can excite kinetic Alfvén waves with a larger growth rate compared to other two cases discussed above. From the above analysis, it was evident that in the presence of a finite shear, the ion-beam streaming should be anti-parallel to the ambient magnetic field to make the condition more favorable for excitation of kinetic Alfvén waves.

In Figures 4a and 4b, the variations of the normalized real frequency and growth rate with λ_B for different β_i values (shown on the curves) are depicted for the plasma parameters of Figure 1 and $V_B/\alpha_B = 0.5$. Here, waves were excited by ion-beam streaming alone. It was seen that the effect of β_i was negligible on the real frequency of the kinetic Alfvén waves. However, the growth rate of the wave decreased with a decrease in β_i without any change in the λ_B range for the set of parameters considered here. It was noticed that the waves were excited for $\lambda_B < 1$.

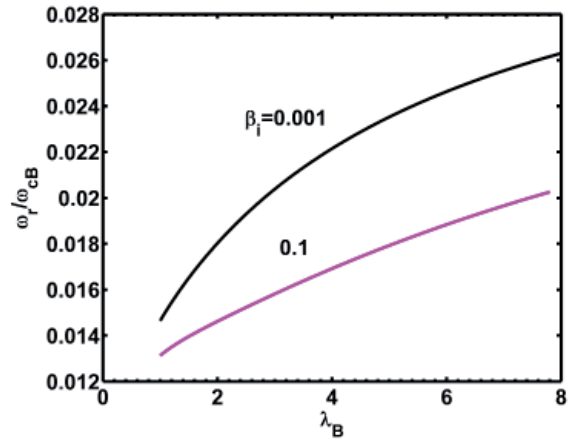

Figure 5a. The resonant instability of kinetic Alfvén waves driven by an ion beam and velocity shear: the normalized real frequency, ω_r/ω_{cB}, as a function of $\lambda_B = \frac{k_\perp^2 \alpha_B^2}{2\omega_{cB}^2}$ for $\frac{N_B}{N_e} = 0.4$, $\frac{V_B}{\alpha_B} = -0.25$, $\frac{k_\parallel}{k_\perp} = 0.04$ $S = 0.4$, and for $\beta_i = 0.001$ and 0.1, respectively.

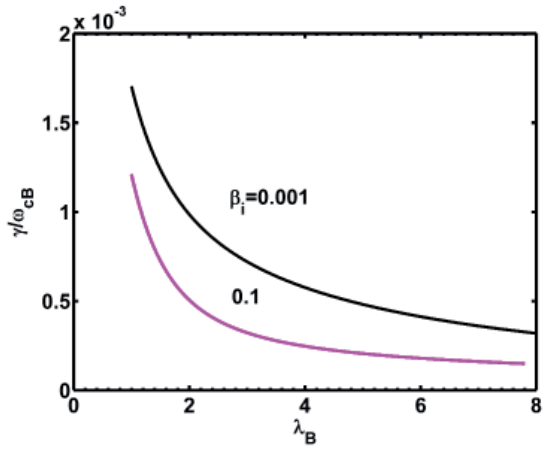

Figure 5b. The resonant instability of kinetic Alfvén waves driven by an ion beam and velocity shear: the normalized growth rate, γ/ω_{cB}, as a function of $\lambda_B = \frac{k_\perp^2 \alpha_B^2}{2\omega_{cB}^2}$ for $\frac{N_B}{N_e} = 0.4$, $\frac{V_B}{\alpha_B} = -0.25$, $\frac{k_\parallel}{k_\perp} = 0.04$ $S = 0.4$, and for $\beta_i = 0.001$ and 0.1, respectively.

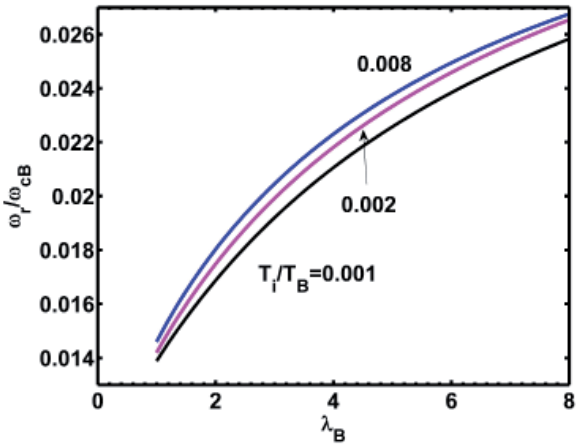

Figure 6a. The resonant instability of kinetic Alfvén waves driven by an ion beam and velocity shear: the normalized real frequency, ω_r/ω_{cB}, as a function of $\lambda_B = \frac{k_\perp^2 \alpha_B^2}{2\omega_{cB}^2}$ for $\frac{N_B}{N_e} = 0.4$, $\frac{V_B}{\alpha_B} = -0.25$, $\frac{k_\parallel}{k_\perp} = 0.04$ $S = 0.4$, $\beta_i = 0.001$, and for $T_i/T_B = 0.001,\ 0.002$, and 0.008, respectively.

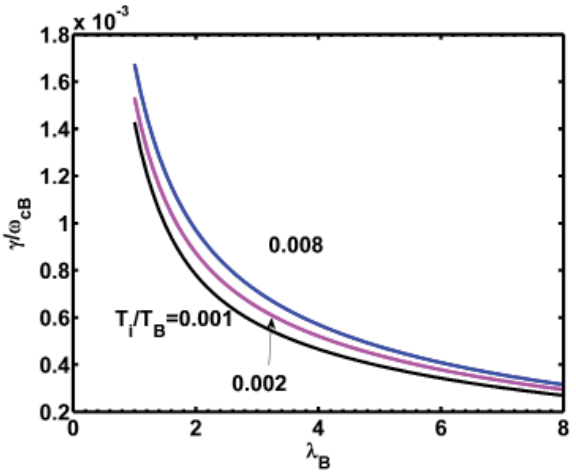

Figure 6b. The resonant instability of kinetic Alfvén waves driven by an ion beam and velocity shear: the normalized growth rate, γ/ω_{cB}, as a function of $\lambda_B = \frac{k_\perp^2 \alpha_B^2}{2\omega_{cB}^2}$ for $\frac{N_B}{N_e} = 0.4$, $\frac{V_B}{\alpha_B} = -0.25$, $\frac{k_\parallel}{k_\perp} = 0.04$ $S = 0.4$, $\beta_i = 0.001$, and for $T_i/T_B = 0.001,\ 0.002$, and 0.008, respectively.

Here we show the effect of β_i on the waves in the presence of both a finite positive shear ($S = 0.4$) and anti-parallel streaming of the ion beam ($\frac{V_B}{\alpha_B} = -0.25$). The normalized real frequency and growth rate are shown in Figures 5a and 5b for values of $\beta_i = 0.001$ and 0.1. Other plasma parameters were as in Figure 3. A significant enhancement was observed in both the real frequency and growth rate with a decrease in the β_i value, and the wave could also grow for a larger range of wave numbers. The decrease in β_i had a reverse effect on the growth rate of kinetic Alfvén waves for the combined case of an ion beam and velocity shear as compared to the ion-beam case alone. In this case, the waves were excited for

In Figures 6a and 6b, we show the effect of the temperature variation, T_i/T_B, on the real frequency and growth rate of kinetic Alfvén waves for the parameters of Figure 3 and $\frac{V_B}{\alpha_B} = -0.25$. The real frequency as well as the growth rate increased with an increase in the temperature's T_i/T_B values.

4. Discussion and Conclusions

This paper discussed a three-component plasma model for the excitation of kinetic Alfvén waves by ion beam and velocity shear. It was observed that an ion beam solely streaming parallel to the ambient magnetic field could excite kinetic Alfvén waves for a significant growth. The ion beam streaming anti-parallel to the ambient magnetic field in the presence of a finite positive shear will also excite kinetic Alfvén waves more efficiently as compared to the ion-beam case alone.

An enhancement in the growth rate of kinetic Alfvén waves was observed with a decrease in β_i value for a combination of anti-parallel streaming ion beam and positive velocity shear, whereas a reverse trend was obtained in the absence of shear and ion-beam streaming parallel to the magnetic field, i.e., a reduction in the growth rate of kinetic Alfvén waves was found. For the case of an ion beam alone, these waves were excited for $\lambda_B < 1$. On the other hand, for the case of combined sources (an anti-parallel ion beam and velocity shear), these waves were excited for $\lambda_B > 1$. An increase in temperature, T_i/T_B, had a positive impact on the real frequency and growth rate of kinetic Alfvén waves, i.e., both increased with an increase in temperature.

For our computational purposes, we considered some typical plasma parameters observed on the auroral/polar-cusp field lines at an altitude of $5R_E$ to $7R_e$, where R_E is the radius of the Earth [22, 23, 31]. The values reported were ion-beam densities $N_B/N_e = (0.01 \text{ to } 0.2)$; beam speed $V_B/\alpha_B < 2$; $\frac{\omega_{cB}}{2\pi} \approx (2.2-3)$ Hz, more common at auroral altitude; whereas we used $N_B/N_e = (0.1 \text{ to } 0.4)$, $V_B/\alpha_B = (-0.5 \text{ to } 0.9)$, $\beta_i = (0.001 \text{ to } 0.1)$, $\frac{\omega_{cB}}{2\pi} = 2.5$ and $S = (0.1 \text{ to } 0.4)$ for our numerical experiments. For the temperature of the species we assumed the following: for the hot electrons, $T_e \approx 100$eV; for the background cold ions, $T_i \approx 10$eV; and for the ion beam, $T_B \approx 1$keV to 2keV.

For the case of the excitation of the kinetic Alfvén waves by the ion beam alone, the normalized peak growth rate was found to be 0.00009 at $\lambda_B = 0.33$, and the corresponding real frequency peak was 0.008, whereas the wave was excited for $\lambda_B = (0.1 \text{ to } 1.5)$. The corresponding un-normalized growth rate and real frequency were 0.00023 Hz and 0.02 Hz, respectively.

The un-normalized real frequency had a range of 10 mHz to 40 mHz, and the corresponding growth rate fell in the range of 0.013 mHz to 0.23 mHz for the whole range of our computations. The transverse wave number was found to be in the range $k_\perp \approx 0.02\text{km}^{-1}$ to 0.04km^{-1}. The corresponding perpendicular wavelength fell in the range 314 km to 157 km. The parallel wave number, which can be obtained from the relation $k_\parallel / k_\perp = 0.04$, was found to be $k_\parallel \approx 0.08\times10^{-2}\,\text{km}^{-1}$ to $0.16\times10^{-2}\,\text{km}^{-1}$, and the parallel wavelength value was 78×10^2 km to 39×10^2 km. In the presence of finite shear and anti-parallel ion-beam streaming, the peak of the normalized growth rate significantly increased in comparison to the ion-beam case alone, and was found to be 0.0018 for $\lambda_B = 1.0$. The corresponding real frequency was found to be 0.015, whereas the kinetic Alfvén waves were excited in the λ_B range of 1.0 to 8.0. The respective un-normalized growth rate and real frequency had values of 0.0045 Hz and 0.04 Hz, respectively. The un-normalized real frequency fell in the range of 37.5 mHz to 65 mHz, and the growth rate had a range of 0.9 mHz to 4.5 mHz. The perpendicular wavenumber was found to be 0.03km^{-1} to 0.10km^{-1}. From this, the perpendicular wave length was obtained to be 209 km to 62 km. The respective parallel wave number was found to be $0.12\times10^{-2}\,\text{km}^{-1}$ to $0.4\times10^{-2}\,\text{km}^{-1}$, which gave the parallel wavelength values as 52×10^2 km to 15×10^2 km. The numerically calculated perpendicular wavelengths of 62 km to 314 km matched well with the observed values of 20 km to 120 km in the auroral region [8].

The theoretical model developed here provides insight into the generation mechanism of kinetic Alfvén waves by an ion beam alone, as well as by both the ion beam and velocity shear. Our model can excite kinetic Alfvén waves up to a frequency of ≈ 10 mHz to ≈ 65 mHz for the auroral-region parameters. It can explain some of the characteristics (perpendicular wavelengths) of observed ULF waves in the Earth's magnetosphere [8].

5. Acknowledgements

GSL thanks the Indian National Science Academy, New Delhi, for the support under INSA-Honorary Scientist Scheme. KCB would like to thank AP-RASC for providing the financial support under the Student Paper Competition (SPC) program to present his results. KCB would also like to thank the Indian Institute of Geomagnetism (IIG) for the financial support to attend the AP-RASC.

6. References

1. A. Hasegawa and L. Chen, "Kinetic Processes in Plasma Heating by Resonant Mode Conversion of Alfvén Wave," *Physics of Fluids*, **19**, 1976, pp. 1924-1934.

2. A. Hasegawa and K. Mima, "Anomalous Transport Produced by Kinetic Alfvén Wave Turbulence," *Journal of Geophysical Research*, **19**, 1978, pp. 1117-1123.

3. C. K. Goertz and R. W. Boswell, "Magnetosphere-Ionosphere Coupling," *Journal of Geophysical Research*, **84**, 1979, pp. 7239.

4. R. L. Lysak, and Christian T. Dum, "Dynamics of Magnetosphere-Ionosphere Coupling Including Turbulent Transport," *Journal of Geophysical Research: Space Physics*, **88.A1**, 1983, pp. 365-380.

5. B. J. Thompson and R. L. Lysak, "Electron Acceleration by Inertial Alfvén Waves," *Journal of Geophysical Research: Space Physics*, **101**, 1996, pp. 5359-5369.

6. A. Hasegawa, "Particle Acceleration by MHD Surface Waves and Formation of Aurora," *Journal of Geophysical Research*, **81**, 1976, pp. 5083.

7. R. L. Lysak and C.W. Carlson, "Effect of Microscopic Turbulence on Magnetosphere and Ionosphere Coupling," *Geophysical Research Letters*, **8**, 1981, pp. 269.

8. J. R. Wygant, A. Keiling, C. A. Cattell, R. L. Lysak, M. Temerin, F. S. Mozer, C. A. Kletzing, J. D. Scudder, V. Streltsov, W. Lotko, et al., "Evidence for Kinetic Alfvén Waves and Parallel Electron Energization at 4-6 R_E Altitudes in the Plasma Sheet Boundary Layer," *Journal of Geophysical Research: Space Physics*, **107** , 2002.

9. C. C. Chaston, L. M. Peticolas, C. W. Carlson, J. P. McFadden , F. Mozer , M. Wilber, G. K. Parks, A. Hull, R. E. Ergun, R. J. Strangeway and M. Andre, "Energy Deposition by Alfvén Waves into the Dayside Auroral Oval: Cluster and FAST Observations," *Journal of Geophysical Research: Space Physics*, **110(A2)**, 2005.

10. C. C. Chaston, G. Vincent , J. W. Bonnell, C. W. Carlson, J. P. McFadden, R. E. Ergun, R. J. Strangeway, E. J. Lund, and K. J. Hwang, "Ionospheric Erosion by Alfvén Waves," *Journal of Geophysical Research: Space Physics*, **111.A3**, 2006.

11. C. C. Chaston, J. W. Bonnell, and C. Salem, "Heating of the Plasma Sheet by Broadband Electromagnetic Waves," *Geophysical Research Letters*, **41.23**, 2014, pp. 8185-8192.

12. T. Izutsu, H. Hasegawa, T. K. M. Nakamura, and M. Fujimoto, "Plasma Transport Induced by Kinetic Alfvén Wave Turbulence," *Physics of Plasmas*, **19.10**, 2012, pp. 102305.

13. D. A. Gurnett, K. L. Huff, D. Menieti, L. Burch, D. Winningham, and S. D. Shawhan, "Correlated Low-Frequency Electric and Magnetic Noise Along Auroral Field Lines," *Journal of Geophysical Research: Space Physics*, **89**, 1984, pp. 8971.

14. A. Berthelier, J-C. Cerisier, J-J. Berthelikr, and L. Rnzeau, "Low-Frequency Magnetic Turbulence in the High-Latitude Topside Ionosphere: Low-Frequency

Waves or Field-Aligned Currents," *Journal of Atmospheric and Terrestrial Physics*, **53.3-4**, 1991, pp. 333-341.

15. J. R. Johnson, and C. Z. Cheng, "Kinetic Alfvén Waves and Plasma Transport at the Magnetopause," *Geophysical Research Letters*, **24.11**, 1997, pp. 1423-1426.

16. J. R. Johnson, C. Z. Cheng, and P. Song, "Signatures of Mode Conversion and Kinetic Alfvén Waves at the Magnetopause," *Geophysical Research Letters*, **28.2**, 2001, pp. 227-230.

17. C. S. Salem, G. G. Howes, D. Sundkvist, S. D. Bale, C. C. Chaston, C. H. K. Chen, and F. S. Mozer, "Identification of Kinetic Alfvén Wave Turbulence in the Solar Wind," *The Astrophysical Journal Letters*, **745.1**, 2012, pp. L9.

18. S. Duan, Z. Liu, and V. Angelopoulos, "Observations of Kinetic Alfvén Waves by THEMIS Near a Substorm Onset," *Chinese Science Bulletin*, **57.12**, 2012, pp. 1429-1435.

19. P. S. Moya, V. A. Pinto, A. F. Viñas, D. G. Sibeck, W. S. Kurth, G. B. Hospodarsky, and J. R. Wygant, "Weak Kinetic Alfvén Waves Turbulence During the 14 November 2012 Geomagnetic Storm: Van Allen Probes Observations," *Journal of Geophysical Research: Space Physics*, **120.7**, 2015, pp. 5504-5523.

20. Daniel J. Gershman, F. Adolfo, John C. Dorelli, Scott A. Boardsen, Levon A. Avanov, Paul M. Bellan, Steven J. Schwartz, et al, "Wave-Particle Energy Exchange Directly Observed in a Kinetic Alfvén-Branch Wave," *Nature Communications*, **8**, 2017, pp. 14719.

21. N. D'Angelo, "Ultralow frequency fluctuations at the polar cusp boundaries," *Journal Geophysical Research*, **78**, 1973, pp. 1206-1209.

22. N. D'Angelo, A. Bahnsen, and H. Rosenbauer, "Wave and Particle Measurements at the Polar Cusp," *Journal Geophysical Research*, **79**, 1974, pp. 3129-3134.

23. D. A. Gurnett and L. A. Frank, "Plasma Waves in the Polar Cusp: Observations from Hawkeye 1," *Journal Geophysical Research: Space Physics*, **83**, 1978, pp. 1447-1462.

24. B. Grison, F. Sahraoui, B. Lavraud, T. Chust, N. Cornilleau-Wehrlin, H. Reme, A. Balogh, and M. Andre, "Wave Particle Interactions in the High-Altitude Polar Cusp: A Cluster Case Study," *Annales Geophysicae*, **23**, 2005, pp. 3699-3713.

25. D. Sundkvist, A. Vaivads, M. Andre, J.-E. Wahlund, Y. Hobara, S. Joko, V. Krasnosel-skikh, Y. Bogdanova, S. Buchert, N. Cornilleau-Wehrlin, et al., "Multi-Spacecraft Determination of Wave Characteristics Near the Proton Gyrofrequency in High-Altitude Cusp," *Annales Geophysicae*, **23**, 2005, pp. 983-995.

26. T. Takada, K. Seki, M. Hirahara, M. Fujimoto, Y. Saito, H. Hayakawa, and T. Mukai, "Statistical properties of low-frequency waves and ion beams in the plasma sheet boundary layer: Geotail observations," *Journal of Geophysical Research: Space Physics*, **110**, 2005.

27. N. D'Angelo, "Plasma Waves and Instabilities in the Polar Cusp: A Review," *Reviews of Geophysics*, **15**, 1977, pp. 299-307.

28. L. Chen and A. Hasegawa, "A Theory of Long-Period Magnetic Pulsations: 1. Steady State Excitation of Field Line Resonance," *Journal of Geophysical Research*, **79**, 1974, pp. 1024-1032.

29. G. S. Lakhina, "Low-Frequency Electrostatic Noise Due to Velocity Shear Instabilities in the Regions of Magnetospheric Flow Boundaries," *Journal of Geophysical Research: Space Physics*, **92**, 1987, pp. 12161-12170.

30. G. S. Lakhina, "Generation of ULF Waves in the Polar Cusp Region by Velocity Shear-Driven Kinetic Alfvén Modes," *Astrophysics and Space Science*, **165**, 1990, pp. 153-161.

31. G. S. Lakhina, "Generation of Kinetic Alfvén Waves by Velocity Shear Instability on Auroral Field Lines," *Advances in Space Research*, **41**, 2008, pp. 1688-1694.

32. David M. Malaspina, Seth G. Claudepierre, Kazue Takahashi, Allison N. Jaynes, Scot R. Elkington, Robert E. Ergun, John R. Wygant, Geoff D. Reeves, and Craig A. Kletzing, "Kinetic Alfvén Waves and Particle Response Associated with a Shock-Induced, Global ULF Perturbation of the Terrestrial Magnetosphere," *Geophysical Research Letters*, **42**, 2015, pp. 9203-9212.

33. D. G. Swanson, *Plasma Waves*, Boca Raton, FL, CRC Press, 075030927X, 2003.

34. K. C. Barik, S. V. Singh, and G. S. Lakhina, "Kinetic Alfvén Waves Generated by Ion Beam and Velocity Shear in the Earth's Magnetosphere," *Physics of Plasmas*, **26.2**, 2019, pp. 022901.